Food Analytical Methods (2024) 17:236–250
https://doi.org/10.1007/s12161-023-02561-x

RESEARCH

Infrared Laser-Based Selected Reaction Monitoring Mass Spectrometry Imaging of Banana (*Musa* spp.) Tissue—New Method for Detection and Spatial Localization of Metabolites in Food

Joanna Nizioł[1] · Maria Misiorek[1] · Zuzanna Krupa[2] · Tomasz Ruman[1]

Received: 19 October 2023 / Accepted: 30 November 2023 / Published online: 13 December 2023

Abstract
In this study, for the first time, we present the application of an infrared (IR) laser ablation-remote-electrospray ionization (LARESI) platform coupled to a tandem mass spectrometer (MS/MS) operated in selected reaction monitoring (SRM) mode for targeted metabolite imaging in intact plant tissues. We examined the distribution of specific metabolites in two banana varieties: Red Dacca and Cavendish. To support MSI results, an extensive analysis of banana tissue extracts was conducted using ultra-high-performance liquid chromatography and ultra-high-resolution mass spectrometry (UHPLC-UHRMS). In the Cavendish banana, 12 metabolites were successfully identified, while Red Dacca bananas were found to contain 16 amino acids. The spatial distribution of some of these compounds found in bananas was presented for the first time. This approach eliminates the need for high vacuum conditions and the pretreatment of biological materials, making it an efficient and promising tool for studying metabolites in plant tissues.

Keywords Mass spectrometry imagining · Laser ablation · Ambient mass spectrometry imaging · Metabolites · Banana

Introduction

Banana (*Musa L.*) stands as a highly favored tropical fruit due to its exceptional nutritional value (Singh et al. 2016a; Qamar and Shaikh 2018; Yun et al. 2022). Banana belongs to the monocot plants in the banana family (*Musaceae Juss.*), and its origins trace back to Southeast Asia. This tropical fruit has garnered attention for its remarkable antioxidant and antimicrobial capabilities, attributed to the presence of widespread polyamines and bioactive amines (Adão and Glória 2005; Lima et al. 2008). Moreover, banana pulp serves as a rich source of valuable nutraceuticals and bioactive compounds, including carbohydrates, amino acids (AAs), carotenoids, polyphenols, and phytosterols (Singh et al. 2016b; Sidhu and Zafar 2018; Maduwanthi and Marapana 2021; Mondal et al. 2021). Banana enjoys the status of being one of the most widely consumed fruits worldwide, not only due to its popularity as a nutritional source but also its significant contribution to the global economy and trade, with many countries depending partially or entirely on their banana production (Hussein et al. 2020). Despite their commercial importance, bananas often encounter challenges from various diseases caused by fungi, bacteria, viruses, nematodes, and insects (Shi Ming et al. 2021). The examination of these plant infections is typically conducted using microscopic techniques. However, determining the spatial distribution of chemical compounds necessitates careful examination of the diseased areas in plant tissues.

To gain deeper insights into the intricate processes within living organisms, the ability to examine the spatial distributions of molecules in biological tissues is of paramount importance. While analytical techniques like conventional liquid chromatography mass spectrometry (LC-MS) (Gedük and Zengin 2021) and gas chromatography mass spectrometry (GC–MS) (Dou et al. 2020) have been proven effective in identifying non-volatile and volatile metabolites, respectively, in plant tissue extracts including banana peels and pulps, they offer averaged information for each compound.

✉ Joanna Nizioł
jniziol@prz.edu.pl

[1] Faculty of Chemistry, Rzeszów University of Technology, 6 Powstańców Warszawy Ave., 35-959 Rzeszów, Poland

[2] Doctoral School of Engineering and Technical Sciences at the Rzeszów University of Technology, 8 Powstańców Warszawy Ave., 35-959 Rzeszów, Poland

Mass spectrometry imaging (MSI) is a powerful analytical tool that provides simultaneous spatial distribution information of up to thousands of molecules in a variety of samples in a single experiment without the necessity for labeling or altering the structure of the original molecules (Stoeckli et al. 2001; Chaurand et al. 2004). This is crucial because labeling interferes with the molecule's properties and behavior or the label itself might react with multiple types of molecules, leading to ambiguous results (McDonnell and Heeren 2007). MSI has been the subject of extensive research in recent decades due to its high sensitivity and ability to precisely quantify the spatial distribution of a variety of chemical compounds in various samples such as tissue sections, which can be of great value in biological research (Gao et al. 2023). Mapping ions on the surface of such specimens can reveal intricate details about how compounds are compartmentalized, the localized metabolic activity, and specific binding regions for an extensive range of both natural and man-made compounds (Caprioli et al. 1997). The undoubted advantage of MSI is that it does not require the homogenization of samples, which is necessary in GC/LC-MS. This means that samples can be analyzed in state close to natural conditions and avoid potential changes to the sample caused by the extraction process. MSI allows the analysis of compounds directly in tissue, which is particularly important in biomedical and pharmacological research, where the location of the compound may be important for its function or toxicity (Cornett et al. 2007). In the case of MSI, samples often require only simple preparation such as freezing and cutting into thin sections with minimal risk of tissue degradation. While LC-MS also allows for the analysis of multiple compounds simultaneously, MSI allows the spatial distribution of multiple compounds to be visualized simultaneously without the need to separate them first (Norris and Caprioli 2013).

MSI can also be useful in quickly assessing food safety (Zou et al. 2022). MSI can detect specific peptides or other biomarkers that are characteristic of specific pathogens with high sensitivity and specificity. Information regarding the location of pathogens in a sample may be crucial to understanding their spread and interactions with food (dos Santos et al. 2017; Rocha et al. 2017). MSI is advantageous for food samples where additional processing may lead to the spread or degradation of pathogens (Araújo et al. 2017).

Among the most commonly utilized techniques for investigating the spatial distribution of compounds in biological samples, matrix-assisted laser desorption ionization (MALDI) (Sarabia et al. 2018), secondary ion mass spectrometry (SIMS) (Eswara et al. 2019), and desorption electrospray ionization (DESI) hold prominence (Yin et al. 2018). These cutting-edge approaches have paved the way for a deeper understanding of the molecular composition and localization within biological systems.

SIMS boasts high efficiency in MS imaging owing to its exceptional sensitivity, highest lateral resolution (10 nm), wide dynamic range, and ability to detect all elements along with their isotope order ($m/z < 1000$) (Audinot et al. 2021). However, known issue with SIMS is moderate-to-heavy fragmentation of compounds of interest. MALDI is a much softer ionization method which enables the determination of compounds with a higher practical mass range (>10,000 Da) but with coarser resolution (30–200 µm).

Nevertheless, both methods require specialized and time-consuming sample preparation. In the MALDI method, thin tissue slices are coated with a matrix solution. However, a significant limitation lies in the need for a laser energy-absorbing matrix solution, which can alter the original spatial distribution of molecules through lateral mixing. Moreover, the requirement for a high vacuum environment restricts the range of materials that can be analyzed using this method, and it is not suitable for in vivo measurements. Furthermore, MALDI may encounter interference from the matrix in the low mass region ($m/z < 1000$), making it challenging to measure the $m/z < 600$ domain (Kaspar et al. 2011; Calvano et al. 2018).

Recent developments in MSI have led to the emergence of ambient ionization techniques, providing new avenues for analyzing biological materials (Wu et al. 2013a; Cabral et al. 2013). DESI stands as one such technique, enabling the imaging of low molecular compounds in plant tissues (Tata et al. 2015). However, DESI has certain limitations, including relatively low spatial resolution (usually around 100–200 µm), low ionization efficiency for specific molecules, and shallow sampling depth, which restricts the amount of material available for analysis. Among ambient environment MS methods, those employing a mid-IR laser for sampling show promise in analyzing metabolites within biological tissues (Bartels and Svatoš 2015). An advantage of using an IR laser is its ability to effectively couple energy into the O–H stretching mode of hydrogen-bonded water, commonly present in hydrated biological materials. This facilitates greater depth of sampling, making it suitable for imaging various tissues including non-flat samples (Joignant et al. 2023).

In recent years, there has been a growing interest in developing MSI technologies to map metabolite abundances in various fruits and vegetables. Researchers have successfully applied MSI to study strawberries and apples (da Silva et al. 2022), rhubarb stalk (Nizioł et al. 2017), and garlic (Misiorek et al. 2017). To the best of our knowledge, there have been only a few published reports investigating banana tissue sections biologically. In a significant milestone in 2007, (Li et al. 2007) conducted MSI of banana tissue using a mid-IR laser at atmospheric pressure without the need for an additional matrix. Instead, naturally occurring water in the biological tissue served as the energy-absorbing matrix. The study primarily focused on water-soluble

components, such as glucose, fructose, sucrose, citric acid, and potassium ions, which were tentatively identified in the thin (0.2–0.5 mm) sections of the banana tissues. However, it is worth noting that the primary focus of the publication was to introduce the new MSI technique. Consequently, it only presented the average mass spectrum from 300 laser shots measured at randomly selected points on the banana tissues. In 2015, Hölscher et al. (2015) used matrix-free Fourier transform ion cyclotron resonance mass spectrometric imaging (LDI-FT-ICR-MSI) for tentative identification of specific low molecular compounds within the red regions of the ornamental banana *Musa acuminata* spp. *Zebrina* cv "Rowe Red." In another study, Wu et al. used gold nanoparticle (AuNP)-immersed paper imprinting MSI strategy to visualize the spatial distribution of some endogenous compounds within banana corms (Wu et al. 2020). More recently, Yin et al. (2022) proposed AuNPs LDI-MSI for investigating the spatiotemporal distribution and metabolite levels within Brazil and Dongguan banana pulps during postharvest senescence.

Despite these remarkable efforts, one of the main challenges in mass spectrometry imaging (MSI) is the difficulty in unambiguously identifying the compounds being imaged. While MSI provides valuable spatial information about the distribution of molecules in a sample, the identification of these molecules can be complex and challenging. To overcome this limitation, tandem mass spectrometry (MS/MS) imaging can be used.

In this work, we present a new approach to molecular imaging of plant tissue based on laser ablation-remote electrospray ionization (LARESI) in selected reaction monitoring (SRM) mode. It was previously used for targeted analysis of metabolites in human tissue (Nizioł et al. 2020) or mycotoxins in infected grains (Szulc and Ruman 2020), enhancing selectivity through compound-specific ion fragmentation in SRM or MRM modes. MS/MS offers high sensitivity, a wide dynamic range, rapid analysis, and suitability for quantitation, making it valuable for the detection and identification of low-molecular-weight compounds. There are no fragmentation-based mass spectrometry imaging results for banana tissue in the literature published to date.

Experimental

Materials and Equipment

Two species of bananas commercially available were selected. One of the species was Red Dacca Banana (*Musa acuminata*), imported from Colombia. The second was the Cavendish banana from the AAA banana cultivar group (*Musa acuminata*). Fresh banana fruits were purchased from local supermarkets. All solvents were of "LC-MS" or analytical reagent grade. High purity deionized water (> 18 MΩ·cm) was produced locally. Optical photographs of tissue samples were obtained on an Olympus SZ10 microscope, equipped with an 8-MP Olympus camera.

Sample Preparation for MSI Analysis

For the LARESI SRM MSI imaging experiments, 100-µm-thick each banana tissue sections were cut using a microtome. The slices were mounted on the Peltier stage set to −18°C to minimize the lateral mixing of compounds in the sample surface. Two different banana tissue sections recovered from two species (Red Dacca and Cavendish Banana) were examined.

Sample Extraction for LC-MS Analysis

Amount of 60 mg of banana tissue was inserted into 2-mL bead beating lysis tubes. Solvent mixture (900 µL of a 1:2 MeOH/$CHCl_3$) was poured into each tissue tube, three glass beads were then added. Bead homogenizer was then used for 45s and then samples were placed on ice. An amount of 120 µl cold water was added to each tube. Homogenization was repeated for 45 s, and after 5 min—for another 45 s. Samples were placed in −20°C for 1 h to precipitate cell debris and protein matter. After this time, centrifugation for 10 min (14000×*g*) was made, upper phases transferred to 130 µL inserts placed in HPLC vials and inserted into a Bruker Elute autosampler. The thermostated chamber of the autosampler was set at 5°C.

LARESI SRM MSI of Bananas

In this study, we employed an Nd/YAG-pumped, tunable OPO laser (IR Opolette 2731-HE; Opotek, Carlsbad, CA, USA) to generate mid-infrared (mid-IR) laser pulses. The laser system produced 4-ns pulses with a maximum repetition frequency of 20 Hz. Specifically, the laser was tuned to emit at a wavelength of 2.94 µm. During experimentation, the pulse energy of the laser was measured to be 3.5 mJ, and this measurement was conducted using a pyroelectric energy meter (PE25-SH-V2; Ophir-Spiricon, Logan, UT, USA).

In our research, we conducted experiments within a controlled environment using an airtight chamber. The chamber was pressurized with nitrogen gas to create a steady stream flowing at a rate of 2 L/min. To maintain optimal conditions for our sample, we placed it on a 50 × 50 mm sample stage within the chamber. The sample was kept at temperatures as low as –18° C through the use of a Peltier cooling plate (TE-127-1.4-1.5; TE Technology, Traverse City, MI, USA). To manage any excess heat generated by the Peltier element, we implemented a circulating water system coupled with an external radiator. The temperature-controlled sample stage

was mounted on a motorized XY-stage (MTS50-Z8; Thorlabs, Newton, NJ, USA) to enable precise movement and positioning. To introduce the laser beam into the sample chamber, we utilized a 1″ Infrasil window (Thorlabs, Newton, NJ, USA), and a gold-plated mirror (PF10-03-M01; Thorlabs) redirected the beam towards the sample stage. A 40-mm focal length CaF_2 spherical lens (Thorlabs, Newton, NJ, USA), mounted on a Z-axis stage (Thorlabs, Newton, NJ, USA), focused the beam onto the sample surface. The incidence angle on the sample was set at 90°, with a laser focus size of 60 ± 10 µm. We measured the pulse energy at the sample surface to be 2.5 mJ. During the imaging process, the laser focal point remained stationary while a computer-controlled XY-stage moved the sample accordingly. To efficiently capture the laser ablation plumes, a funnel connected to a 4-mm I.D. PTFE tube was positioned over the laser ablation site. The pressurized chamber facilitated the entrainment of the laser ablation plumes into the gas, which was then transported to the electrospray ionization (ESI) source of the SCIEX QTRAP 5500 mass spectrometer. For smooth operation and consistent flow, we employed a binary HPLC pump (Agilent G1312A) to provide a steady stream of binary solvent mixture (2:1 IPA:water with 0.5% acetic acid; 20 µL/min) to the electrospray needle. The configuration of this system for LARESI SRM MSI was previously illustrated in our publication, where we successfully applied this method for imaging kidney tissue (Nizioł et al. 2020) and grains (Szulc and Ruman 2020).

To maintain stable conditions for our samples during analysis, we utilized a Peltier module, which kept the samples at a consistent temperature of −18°C. The imaging process focused on square or rectangular areas, encompassing approximately 1 cm^2. With an impressive pixel count of around 1.5×10^3, the spatial resolution ranged from 175 to 300 µm. Each pixel was subjected to the laser for precisely 2 s, and the laser pulse repetition rate was set at 15 Hz. To achieve comprehensive coverage, the sample stage moved at a speed of 2 mm/s between pixels. During the time delay between pixels, which lasted for 4 s, the stage moved along a straight line to position the next pixel accurately. Additionally, there was a time delay of 5 s between lines, ensuring proper alignment during imaging. The total analysis time for an image with an area of 40 × 40 pixels was approximately 3 h excluding tuning and calibration of mass spectrometer. The advanced control and analysis software used in this study have been recently described, guaranteeing reliable and efficient data processing (Brauer et al. 2015).

In MSI analysis, we employed the SCIEX QTRAP 5500 mass spectrometer, operating in positive ion mode, specifically using the SRM measurement mode with Q1/Q3/DP/EP/CE and CXP settings. During SRM mode, we monitored each compound-specific fragmentation for a duration of 10 ms, with a 5-ms delay before monitoring the subsequent fragmentation. This precise timing ensured accurate and comprehensive data acquisition for our analysis. For the ESI source, we set the source temperature at 500°C, with a curtain gas pressure of 20 psi. Additionally, ion source gas 1 was set to 30 psi, while ion source gas 2 was maintained at 20 psi. For positive ion mode, we applied an ion-spray voltage of +5500 V, and for negative mode, it was adjusted to −4500 V. To facilitate collision-induced dissociation, we utilized nitrogen gas as the collision gas, setting it to medium pressure. Detailed settings are presented in Table 1.

UHPLC-Q-ToF-UHRMS of Banana Extracts

UHPLC-Q-ToF-UHRMS analysis was conducted with Bruker Elute UHPLC system operated with Hystar 3.3 software, coupled with a Bruker Impact II mass spectrometer of ESI QToF-MS type (60,000+ resolution version) from Bruker Daltonik GmbH (Bremen, Germany). The UHPLC column used was the Bruker Intensity Solo with C18 silica modification, containing 2-µm particles and having dimensions of 100 × 2.1 mm (length × diameter). To maintain consistent conditions, the UHPLC column was thermostated at 40°C throughout the analysis. For mobile phases, we utilized water with 0.1% HCOOH as phase A and acetonitrile with 0.1% HCOOH as phase B. The injection volume was set at 5 µL, and the percentage of phase B varied as follows: 1% (0–2 min), 99% (17–20 min), and 1% (20.1–30 min). The solvent flow rate was 0.25 mL/min from 0 to 20 min and gradually increased to 0.35 mL/min from 20.1 to 30 min. Internal calibration was carried out using ions from 10 mM sodium formate pumped into the ESI ion source with a syringe pump at an infusion flow rate of 0.12 mL/h (solvent:water:isopropanol 1:1 v/v). High-precision calibration (HPC) mode in Metaboscape was used for the calibration process. The instrument operated in autoMSMS mode, with the *m/z* range set at 50–1500, and the collision-induced dissociation (CID) energy value was maintained at 30 eV. Specific CID settings included an absolute area threshold of 5000 cts, active exclusion 2, and an isolation window for m/z ranges of 100–4, 300–5, 500–6, and 1000–8. For untargeted annotations, we used Metaboscape (ver. 2022b) with a criterion of mass deviation ($\Delta m/z$) under 2 ppm and a mSigma value under 30. MS/MS spectra were automatically matched against MS/MS libraries, such as the Bruker HMDB 2.0 library (with retention times) and the MoNA library (MassBank of North America (MoNA).

Results and Discussion

The MSI method we used in food analysis is a promising technology that, unlike traditional analytical methods such as GC/LC-MS, enables the exact location of various

Table 1 Selected metabolites found in bananas with LARESI-SRM-MSI experiments

No.	Compound name	Plant tissue	Structure	m/z[a]	MS ionization mode	Q1 [*m/z*]	Q3 [*m/z*]	Scan time [ms]	DP [V]	EP [V]	CE [V]	CXP [V]	Ion image
1	Caffeic acid[b]	Cavendish banana	$C_9H_8O_4$	180.0423	Negative	179.0	135.0	5	−48	−8	−21	−11	Fig. 1I
2	Catechin[b]		$C_{15}H_{14}O_6$	290.0790	Negative	289.0	203.0	5	−110	−10	−29	−8	Fig. 1L
					Positive	291.0	139.0	5	16	10	21	10	Fig. 1M
3	Eugenol[b]		$C_{10}H_{12}O_2$	164.0837	Negative	163.0	148.0	5	−49	−5	−19	−13	Fig. 1H
4	Ferulic acid[b,d]		$C_{10}H_{10}O_4$	194.0579	Negative	193.0	134.0	5	−58	−5	−23	−9	Fig. 1J
5	Isobutyl butyrate[b]		$C_8H_{16}O_2$	144.1150	Positive	145.1	71.0	5	70	10	40	10	Fig. 1F
6	Myricetin[b]		$C_{15}H_{10}O_8$	318.0376	Negative	317.0	151.0	20	−20	−10	−26	−8	Fig. 1O
7	Protocatechuic acid[b]		$C_7H_6O_4$	154.0266	Negative	153.0	109.0	5	−64	−5	−22	−9	Fig. 1G
8	Pyruvic acid[b]		$C_3H_4O_3$	88.0160	Negative	87.0	32.0	5	−50	−10	−28	−9	Fig. 1D
					Negative	87.0	43.0						Fig. 1E
9	Quercetin[b]		$C_{15}H_{10}O_7$	302.0427	Negative	301.0	150.9	5	−120	−10	−28	−11	Fig. 1N
10	Sinapic acid[b]		$C_{11}H_{12}O_5$	224.0685	Negative	223.0	192.9	5	−48	−8	−21	−11	Fig. 1K
11	Alanine[b,c]	Red Dacca Banana	$C_3H_7NO_2$	89.0477	Positive	90.1	44.0	30	6	4.5	17	6	Fig. 2C
12	Arginine[b,c,d]		$C_6H_{14}N_4O_2$	174.1117	Positive	133.1	74.0	30	40	11	27	8	Fig. 2O
13	Asparagine[b,c,d]		$C_4H_8N_2O_3$	132.0535	Positive	175.2	70.0	30	50	10	20	15	Fig. 2I
14	Cysteine[b]		$C_3H_7NO_2S$	121.0198	Positive	241.2	152.0	30	20	14	19	10	Fig. 2R
15	Glutamic acid[b]		$C_5H_9NO_4$	147.0532	Positive	148.1	84.0	50	21	14.5	21	10	Fig. 2K
16	Histidine[b,c,d]		$C_6H_9N_3O_2$	155.0695	Positive	156.1	110.0	50	16	13	19	12	Fig. 2M
17	Isoleucine[b]		$C_6H_{13}NO_2$	131.0946	Positive	132.1	69.0	30	8	14.5	23	8	Fig. 2H
18	Lysine[b,c]		$C_6H_{14}N_2O_2$	146.1055	Positive	147.1	84.0	30	15	13.5	23	10	Fig. 2J
19	Methionine[b,d]		$C_5H_{11}NO_2S$	149.0511	Positive	150.2	104.0	50	6	12	15	12	Fig. 2L
20	Phenylalanine[b,d,e]		$C_9H_{11}NO_2$	165.0790	Positive	166.1	103.0	30	11	14	37	12	Fig. 2N
21	Proline[b,c,d]		$C_5H_9NO_2$	115.0633	Positive	116.1	70.0	30	20	13.5	21	10	Fig. 2E
22	Serine[b,c,d]		$C_3H_7NO_3$	105.0426	Negative	106.1	60.0	30	6	10.5	15.5	7	Fig. 2D
23	Threonine[b]		$C_4H_9NO_3$	119.0582	Positive	120.1	103.2	30	105	14.5	25	7	Fig. 2G
24	Tryptophan[b]		$C_{11}H_{12}N_2O_2$	204.0899	Positive	205.1	146.0	30	75	10	25	15	Fig. 2Q
25	Tyrosine[b,d,e]		$C_9H_{11}NO_3$	181.0739	Positive	182.1	165.0	30	20	11	13	8	Fig. 2P
26	Valine[b,d,e]		$C_5H_{11}NO_2$	117.0790	Positive	118.1	55.0	30	11	13.5	27	8	Fig. 2C

CE collision energy, *CXP* cell exit potential, *DP* declustering potential, *EP* entrance potential, *m/z* mass-to-charge ratio, *V* volts, *Q* precursor/parent ion

[a]Theoretical monoisotopic mass

[b]The metabolites identified by high precursor mass accuracy

[c]The metabolites identified by matching retention time

[d]The metabolites identified by matching isotopic pattern

[e]The metabolites identified by matching MS/MS fragment spectra

important plant metabolites such as antioxidants in different sections of plant tissue. This spatial information is critical for understanding how these compounds are dispersed in fruit, which may be useful for basic research as well as enhancing food processing and storage strategies. Unlike extraction methods, MSI can frequently be conducted with minimum sample preparation. This decreases the possibility of sensitive antioxidant chemicals degrading during preparation and avoids potential changes in their natural form during extraction methods. To detect specific antioxidants, traditional quantification may necessitate the use of labels or probes, which can interfere with the compound's activity or modify its concentration. MSI is a label-free technology, which means that it can identify antioxidants in their natural state. MSI provides researchers with not only qualitative but also quantitative data, allowing them to evaluate not only the presence but also the concentration of antioxidants in the geographical context of banana tissue. MSI can capture a comprehensive image of all available antioxidants in a single scan, which can be faster than approaches that require sequential analysis of individual compounds, depending on the setup and the exact MSI technology employed. There is a possibility of losing some molecules or converting them into other ones during traditional extraction and measurement. MSI evaluates chemicals directly in the tissue, lowering these hazards (Yoshimura et al. 2016).

In this publication, we showcased the potential of targeted analysis of low molecular weight compounds (LMWC) through LARESI-MSI in SRM modes, directly applied to intact plant tissues. One of the main advantages of this method is atmospheric pressure ionization that allows for the direct analysis of native or frozen samples without the need for extensive sample preparation or vacuum conditions. This is particularly important for tissue imaging, as it enables researchers to study the spatial distribution of various molecules, including metabolites, lipids, and proteins, without altering their native distribution within the tissue (Wu et al. 2013a). This also makes it possible to perform real-time imaging, providing dynamic information about molecular distributions and changes over time without the need for labeling or staining (Xiao et al. 2020).

The LARESI-SRM-MSI method offers a notable advantage in terms of its straightforward and efficient sample preparation. With this technique, a fragment of the object, measuring up to 5 × 5 cm, is required to be placed directly in the instrument's chamber, eliminating the need for additional coating with MALDI matrix. This streamlined approach simplifies the process, saving time and reducing the risk of introducing artifacts that could alter the sample's original composition (Dong et al. 2016b).

The option of cooling tissue samples is of considerable importance in tissue analysis (Goodwin 2012). In the LARESI method, the tissue sample is securely mounted on the Peltier stage, which can be set to a temperature of −18 °C. This cooling capability offers several advantages during the analysis process. Firstly, it helps to preserve the integrity of the biological material, minimizing any potential degradation or changes in the molecular composition that could occur at higher temperatures. Secondly, the cooling of the tissue sample can slow down metabolite diffusion and thus enhance the spatial resolution and sensitivity of the analysis, allowing for more precise and accurate imaging of the molecules within the tissue.

The key advantage of this method lies in its utilization of a mid-IR laser for the analysis of biological material. Firstly, the IR laser provides enhanced sampling depth, allowing researchers to analyze molecules deeper within the tissue, thereby providing a more comprehensive understanding of the molecular composition (Wu et al. 2013a). Mid-IR lasers with a wavelength around 2.94 µm can effectively couple their energy into the O–H stretching mode of hydrogen-bonded water, which is present in hydrated biological materials. This results in a greater depth of sampling, allowing for analysis of molecules deeper within the tissue, up to about 10 µm for a single laser pulse. Secondly, the IR laser ablation is a non-destructive technique, preserving the integrity of the biological material during analysis and enabling researchers to study the spatial distribution of compounds without altering their native state. Additionally, the IR laser offers high sensitivity and selectivity, allowing for the targeted analysis of specific compounds of interest, while reducing chemical noise (Wu et al. 2013a).

For our study, we utilized commercially available banana tissue slices as the sample material. Figures 1 and 2 depict ion images of 26 selected metabolites found in slices of Cavendish banana and Red Dacca Banana tissue, respectively. Mass spectrometry parameters of LARESI SRM MSI Experiments are listed in Table 1. To further validate the MSI results, an extensive analysis of banana tissue extracts was conducted using ultra-high-performance liquid chromatography and ultra-high-resolution mass spectrometry (UHPLC-UHRMS). The untargeted results of the analysis of banana extracts are listed in Table 2.

Bananas are known for being abundant in various compounds found in the plant world, such as phenolic and polyphenolic substances like catechin, myricetin, quercetin, and phenolic acids like caffeic, protocatechuic acid, ferulic acid, and sinapic acids. Additionally, volatile compounds like isobutyl butyrate, eugenol, and pyruvic acid, representing alpha-keto acids, are also present in significant quantities. Phenolics and polyphenolics are the dominant compounds in banana fruits, and they are widespread throughout the plant kingdom. These secondary metabolites are of utmost importance due to their various health benefits, including antioxidant, antimicrobial, anti-inflammatory, anticancer, anti-mutagenic, and antidiabetic properties. The profiling

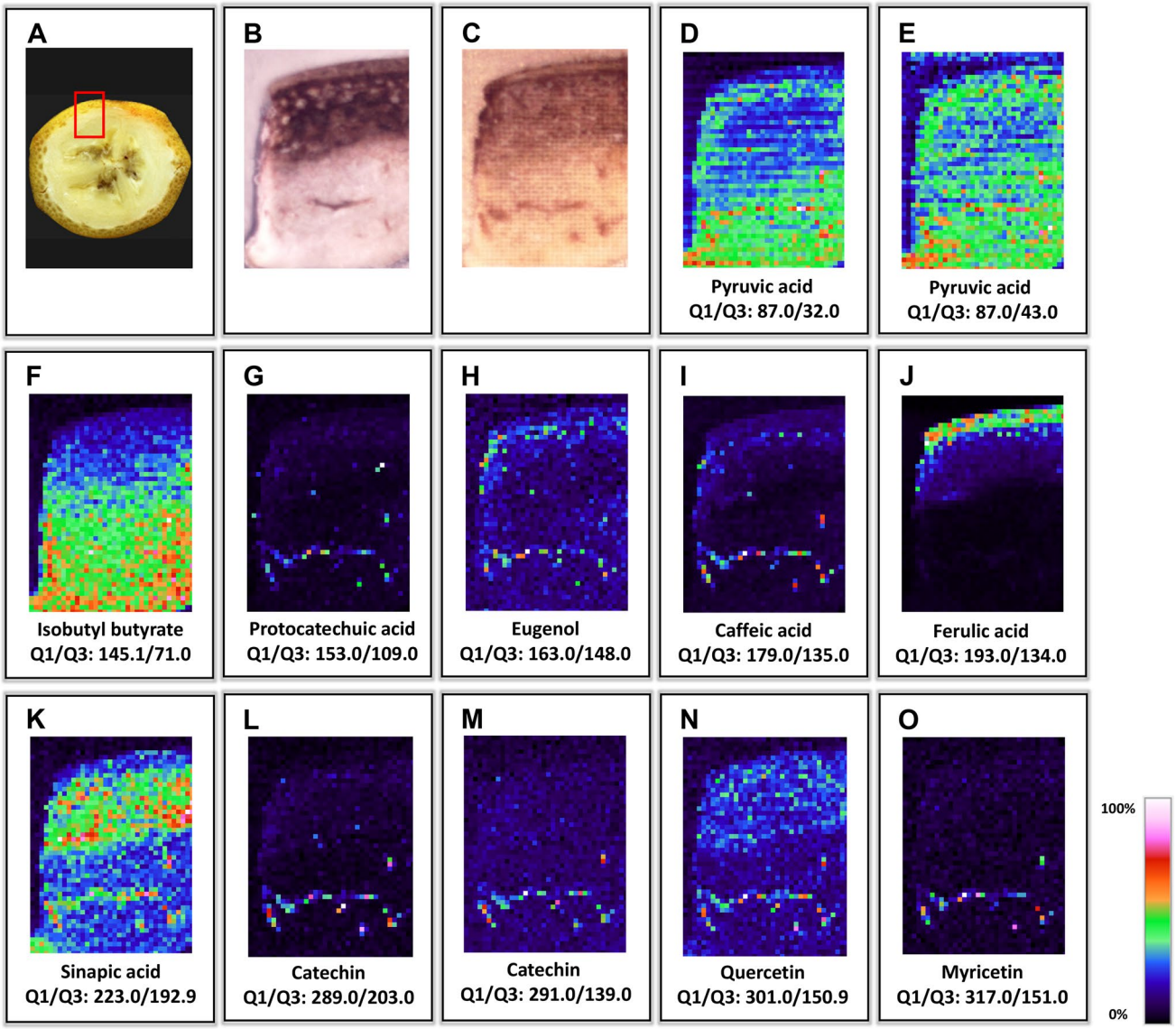

Fig. 1 Photographs and LARESI SRM MSI ion images of selected metabolites in the Cavendish banana tissue section. Optical photographs of the imaged surface of the banana tissue before (**A**, **B**) and following imaging (**C**). LARESI SRM MSI ion images of the Cavendish banana tissue (**D**–**O**). The imaged area is 8 × 8 mm obtained with 40 × 40 pixels and at 200 × 200 µm resolution

of phenolic compounds in different banana varieties was carried out using HPLC–ESI-HR-MS and HPLC-DAD methods (Simirgiotis et al. 2013; Tongkaew et al. 2022). The research findings indicate that bananas serve as an excellent source of phenolic compounds, although their content can vary in different parts of the fruit, such as the pulp and peel.

Among the compounds under analysis, phenolic acids played a prominent role, including protocatechuic acid, caffeic acid, ferulic acid, and sinapic acid. Protocatechuic acid, classified as a dihydroxybenzoic acid, is a naturally occurring phenolic acid widely distributed across the plant kingdom, alongside other plant phenols. In previous studies, both protocatechuic acid and caffeic acid were successfully identified in acetone banana pseudostem extracts using reverse-phase HPLC and ESI-MS, indicating their presence in this plant tissue (Saravanan and Aradhya 2011). Furthermore, quantification of these compounds was performed in banana rhizome extracts from eight commercial banana cultivars, with protocatechuic acid identified as the primary phenolic compound in acetone extracts of banana rhizomes (Kandasamy and Aradhya 2014) Caffeic acid, a common cinnamic acid derivative, is renowned for its antioxidant and antimicrobial properties and was also detected in banana peel extracts using paper spray-mass spectrometry in separate studies (Vu et al. 2018; Silva et al. 2020).

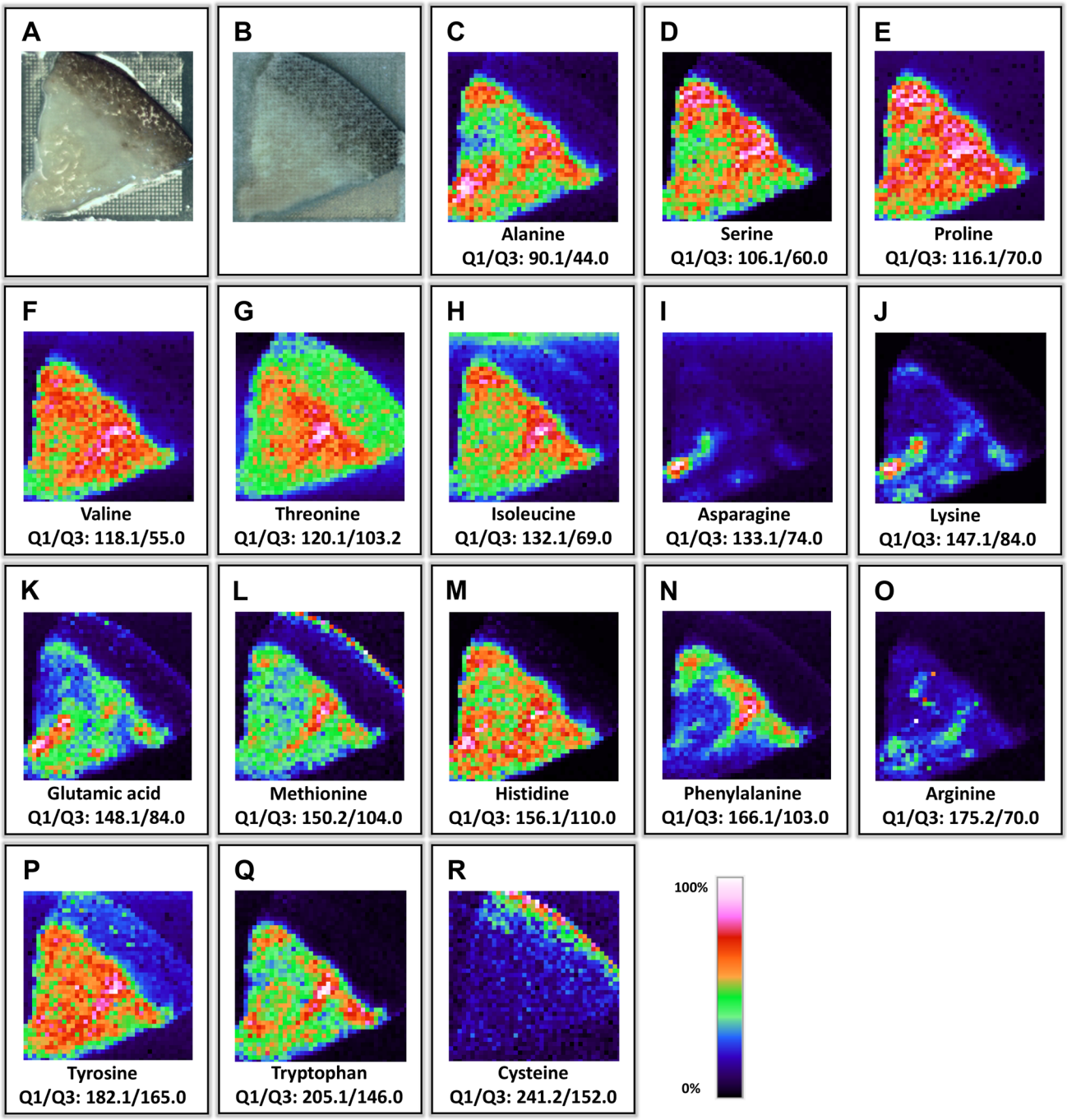

Fig. 2 Photographs and LARESI SRM MSI ion images of selected amino acids in intact Red Dacca Banana tissue section. Optical photographs of the imaged surface of the banana tissue before (**A**) and following imaging (**B**). LARESI SRM MSI ion images of the Red Dacca Banana tissue (**C**–**R**). The imaged area is 12×12 mm obtained with 40 × 40 pixels and at 300 × 300 µm resolution

Bananas are renowned for being rich in compounds with valuable medicinal properties, including ferulic acid. As a phenolic acid and derivative of cinnamic acid, ferulic acid is widely distributed throughout the plant kingdom, naturally occurring in plant cell walls, notably in conifers' leaves, seeds, and bark, as well as in grains like wheat, rice, corn, and rye. The significance of ferulic acid extends to various beneficial biological activities, especially for human health, such as its role as an antioxidant, antimicrobial, anti-inflammatory, anticancer, anti-mutagenic, and antidiabetic agent. Its widespread applicability is reflected in its use across the food, cosmetics, and pharmaceutical industries, owing to its

Table 2 Metabolite identification in Cavendish banana extract using UHPLC-UHRMS Method

No.	Name	Molecular Formula	*m/z*[a]	RT [min]	Ions	Δ*m/z* [ppm]
1	3-Hydroxybutyric acid[b,d]	$C_4H_8O_3$	146.0812	1.10	$[M+H]^+$, $[M+H+CH_3CN]^+$	0.5
2	2,3-Butanediol[b,d]	$C_4H_{10}O_2$	132.1016	18.11	$[M+H]^+$, $[M+H+CH_3CN]^+$	−2.0
3	2-Hydroxyacetanilide[b,d,e]	$C_8H_9NO_2$	152.0703	17.75	$[M+H]^+$	−2.1
4	2-Octenoic acid[b,c]	$C_8H_{14}O_2$	184.1330	17.88	$[M+H]^+$	−1.3
5	2-Oxoarginine[b,d]	$C_6H_{11}N_3O_3$	174.0871	8.45	$[M+H]^+$	−1.2
6	3-Hydroxy-4-methoxycinnamic aicd[b,d]	$C_{10}H_{10}O_4$	236.0912	0.97	$[M+H]^+$	−1.9
7	4-Ethylbenzoic acid[b,c]	$C_9H_{10}O_2$	151.0750	3.94	$[M+H]^+$	−2.4
8	4-Methylcatechol[b,d]	$C_7H_8O_2$	166.0860	0.72	$[M+H+CH_3CN]^+$, $[M+NH_4]^+$	−1.7
9	5α-Androstane-3β,17β-diol[b,d]	$C_{19}H_{32}O_2$	310.2736	8.43	$[M+H]^+$	−2.1
10	5-Aminopentanoate[b,d,e]	$C_5H_{11}NO_2$	118.0861	3.17	$[M+H]^+$	−1.4
11	6-(Methylamino)purine[b]	$C_6H_7N_5$	150.0772	1.64	$[M+H]^+$	−1.8
12	6-Phosphogluconic acid[b,c]	$C_6H_{13}O_{10}P$	277.0318	2.28	$[M+H]^+$	−0.4
13	Acetic acid[b,d]	$C_2H_4O_2$	102.0548	2.89	$[M+H]^+$	−1.2
14	Adenosine[b,d,e]	$C_{10}H_{13}N_5O_4$	268.1033	1.76	$[M+H]^+$, $[M+Na]^+$	−2.3
15	Biotin[b,d]	$C_{10}H_{16}N_2O_3S$	245.0948	0.98	$[M+H]^+$	−1.7
16	Butanal[b,d]	C_4H_8O	114.0910	2.05	$[M+H]^+$	−2.7
17	Cellobiose[b,c,d]	$C_{12}H_{22}O_{11}$	360.1495	5.57	$[M+NH_4]^+$, $[M+H-H_2O]^+$, $[M+H]^+$	−1.5
18	Cytidine[b,c,d]	$C_9H_{13}N_3O_5$	307.1020	6.42	$[M+H]^+$	2.1
19	Alanine[b,c]	$C_3H_7NO_2$	90.0549	6.57	$[M+H]^+$	−0.8
20	Galactose[b,c,d]	$C_6H_{12}O_6$	203.0528	1.17	$[M+H]^+$	0.8
21	Glucose[b,c,d]	$C_6H_{12}O_6$	219.0262	7.93	$[M+H]^+$	−1.9
22	Dimethylglycine[b,c,d]	$C_4H_9NO_2$	142.0261	1.63	$[M+H]^+$	−0.2
23	Maltose[b,c,d]	$C_{12}H_{22}O_{11}$	381.0788	1.15	$[M+H]^+$	−1.8
24	Dodecanoic acid[b,c]	$C_{12}H_{24}O_2$	242.2108	1.07	$[M+H]^+$	−2.8
25	Epigallocatechin[b,d,e]	$C_{15}H_{14}O_7$	307.0805	1.11	$[M+H]^+$	−2.3
26	Erythrose[b]	$C_4H_8O_4$	162.0759	2.33	$[M+H]^+$	−1.3
27	Ethyl isopropyl ketone[b]	$C_6H_{12}O$	139.0517	1.10	$[M+H]^+$	−2.1
28	Formamide[b]	CH_3NO	125.0109	1.41	$[M+H]^+$	−1.9
29	Fructose 6-phosphate[b,c]	$C_6H_{13}O_9P$	298.9925	1.81	$[M+H]^+$	−1.2
30	Glutamylcysteine[b,d]	$C_8H_{14}N_2O_5S$	251.0695	0.98	$[M+H]^+$	−0.9
31	Glycerol[b,c]	$C_3H_8O_3$	134.0812	1.06	$[M+H]^+$	0.1
32	Glycerophosphocholine[b,c,d]	$C_8H_{20}NO_6P$	296.0656	8.09	$[M+H]^+$	−1.2
33	Guanidine[b,d]	CH_5N_3	139.0384	1.84	$[M+H]^+$	2.5
34	Heptadecanoic acidb	$C_{17}H_{34}O_2$	293.2457	1.10	$[M+H]^+$	2.0
35	Homogentisic acid[b,d,e]	$C_8H_8O_4$	169.0490	1.14	$[M+H]^+$	−3.0
36	Imidazole[b,c,d]	$C_3H_4N_2$	110.0711	1.17	$[M+H]^+$	−1.7
37	Indolelactic acid[b,c,d]	$C_{11}H_{11}NO_3$	206.0814	6.31	$[M+H]^+$	0.0
38	Isobutyric acid[b,c]	$C_4H_8O_2$	89.0595	1.17	$[M+H]^+$	−2.6
39	Isocitric acid[b,c,d]	$C_6H_8O_7$	210.0607	1.15	$[M+H]^+$	−0.7
40	Arginine[b,c,d]	$C_6H_{14}N_4O_2$	213.0746	1.31	$[M+H]^+$	−1.0
41	Asparagine[b,c,d]	$C_4H_8N_2O_3$	133.0607	17.87	$[M+H]^+$	−0.7
42	Aspartic acid[b,c]	$C_4H_7NO_4$	134.0447	1.20	$[M+H]^+$	−1.0
43	Levoglucosan[b,d]	$C_6H_{10}O_5$	163.0598	1.74	$[M+H]^+$, $[M+H-H_2O]^+$, $[M+NH_4]^+$	−1.8
44	Fucose[b,d]	$C_6H_{12}O_5$	206.1006	1.03	$[M+H]^+$	−1.3
45	Glutamine[b,c,d]	$C_5H_{10}N_2O_3$	147.0762	1.18	$[M+H]^+$	−1.4
46	Histidine[b,c,d]	$C_6H_9N_3O_2$	194.0326	5.69	$[M+H]^+$	−0.3
47	Linoleic acid[b,d]	$C_{18}H_{32}O_2$	298.2731	1.03	$[M+NH_4]^+$, $[M+Na]^+$	−2.6
48	Lysine[b,c]	$C_6H_{14}N_2O_2$	147.1128	1.01	$[M+H]^+$	−0.3
49	Malic acid[b,c]	$C_4H_6O_5$	152.0551	1.11	$[M+H]^+$	−1.8
50	LPC(16:1)[b,d,e]	$C_{24}H_{48}NO_7P$	494.3218	1.10	$[M+H]^+$	−4.7

Table 2 (continued)

No.	Name	Molecular Formula	*m/z*[a]	RT [min]	Ions	Δ*m/z* [ppm]
51	LPC(18:2)[b,d,e]	$C_{26}H_{50}NO_7P$	520.3374	1.01	$[M+H]^+$, $[M+Na]^+$	−4.5
52	LPC(18:3)[b,d,e]	$C_{26}H_{48}NO_7P$	518.3218	19.70	$[M+H]^+$	−4.5
53	Proline[b,c,d]	$C_5H_9NO_2$	116.0705	1.10	$[M+H]^+$	−1.3
54	Serine[b,c,d]	$C_3H_7NO_3$	106.0496	19.09	$[M+H]^+$	−2.1
55	Sorbose[b,c,d]	$C_6H_{12}O_6$	163.0598	17.44	$[M+H\text{-}H_2O]^+$, $[M+H]^+$	−1.7
56	Mannose 6-phosphate[b,c,d]	$C_6H_{13}O_9P$	261.0367	8.12	$[M+H]^+$	−1.4
57	Methionine[b,d]	$C_5H_{11}NO_2S$	191.0849	1.09	$[M+H]^+$	0.2
58	Trimethyllysine[b,d,e]	$C_9H_{20}N_2O_2$	189.1596	16.38	$[M+H]^+$	−1.1
59	Oenanthic ether[b,c,d]	$C_9H_{18}O_2$	200.1640	13.15	$[M+H]^+$	−2.1
60	Oxoglutaric acid[b,c]	$C_5H_6O_5$	147.0287	12.93	$[M+H]^+$	−0.9
61	Pantothenic acid[b,d]	$C_9H_{17}NO_5$	220.1174	7.39	$[M+H]^+$, $[M+Na]^+$	−2.5
62	Coumaric acid[b,d,e]	$C_9H_8O_3$	165.0542	1.12	$[M+H]^+$	−2.4
63	Pentadecanoic acid[b,d]	$C_{15}H_{30}O_2$	243.2311	1.16	$[M+H]^+$	−1.9
64	Phenylacetaldehyde[b,d,e]	C_8H_8O	121.0646	1.08	$[M+H]^+$, $[M+NH_4]^+$	−1.6
65	Phenylacetic acid[b,d,e]	$C_8H_8O_2$	137.0594	10.51	$[M+H]^+$, $[M+NH_4]^+$, $[M+H\text{-}H_2O]^+$	−2.3
66	Phenylalanine[b,d,e]	$C_9H_{11}NO_2$	166.0858	15.53	$[M+H]^+$, $[M+Na]^+$	−2.8
67	Phenylglyoxylic acid[b,c]	$C_8H_6O_3$	168.0658	0.90	$[M+H]^+$	1.8
68	Phosphocreatine[b,d]	$C_4H_{10}N_3O_5P$	253.0704	1.02	$[M+H]^+$	3.0
69	Propyl alcohol[b]	C_3H_8O	102.0911	1.10	$[M+H]^+$	−2.5
70	Propylene glycol[b,c,d]	$C_3H_8O_2$	118.0861	1.12	$[M+H]^+$	−1.5
71	Putrescine[b,c]	$C_4H_{12}N_2$	89.1073	11.50	$[M+H]^+$	−0.6
72	Pyridoxamineb	$C_8H_{12}N_2O_2$	169.0969	0.93	$[M+H]^+$	−1.7
73	Pyroglutamic acid[b,c,d]	$C_5H_7NO_3$	130.0497	1.23	$[M+H]^+$	−1.6
74	Pyruvaldehyde[b]	$C_3H_4O_2$	114.0548	1.09	$[M+H]^+$	−1.7
75	Quinic acid[b,c]	$C_7H_{12}O_6$	193.0705	1.09	$[M+H]^+$	−0.7
76	Quinone[b,c,d]	$C_6H_4O_2$	109.0283	1.21	$[M+H]^+$	−0.8
77	Raffinose[b,d,e]	$C_{18}H_{32}O_{16}$	522.2032	5.52	$[M+H]^+$	−2.2
78	Raffinose[b,c,d]	$C_{18}H_{32}O_{16}$	543.1313	6.52	$[M+NH_4]^+$, $[M+Na]^+$	−1.9
79	Rhamnose[b,c]	$C_6H_{12}O_5$	206.1021	1.76	$[M+H]^+$	−0.8
80	Salicinb	$C_{13}H_{18}O_7$	309.0938	1.09	$[M+H]^+$	−2.2
81	Salsolinol[b,d,e]	$C_{10}H_{13}NO_2$	180.1015	7.30	$[M+H]^+$	−2.5
82	Senecioic acid[b,c,d]	$C_5H_8O_2$	118.0858	0.87	$[M+H]^+$	−2.8
83	Methylmethionine[b,d,e]	$C_6H_{13}NO_2S$	164.0738	19.73	$[M+H]^+$	−1.0
84	Succinic acid semialdehyde[b,d]	$C_4H_6O_3$	85.0285	14.61	$[M+H\text{-}H_2O]^+$, $[M+NH_4]^+$	1.0
85	Sucrose[b,d,e]	$C_{12}H_{22}O_{11}$	360.1494	1.72	$[M+NH_4]^+$, $[M+H]^+$, $[M+H\text{-}H_2O]^+$	−2.0
86	Trehalose[b,c,d]	$C_{12}H_{22}O_{11}$	365.1047	1.76	$[M+H]^+$	−2.2
87	Tyrosine[b,d,e]	$C_9H_{11}NO_3$	182.0809	8.84	$[M+H]^+$	−1.9

m/z mass-to-charge ratio, *RT* retention time

[a]Experimental monoisotopic mass

[b]The metabolites identified by high precursor mass accuracy

[c]The metabolites identified by matching retention time

[d]The metabolites identified by matching isotopic pattern

[e]The metabolites identified by matching MS/MS fragment spectra

low toxicity and numerous health benefits (Zduńska et al. 2018) Notably, ferulic acid's potent antioxidant properties surpass even those of vitamins C and E. Previous studies have involved the mechanical extraction of ferulic acid from banana stem waste, aiming to determine kinetic parameters in the production of this compound using HPLC. In our study, ferulic acid is primarily found in the outer part of the banana peel (Fig. 1J). The presence of ferulic acid in the peel of a banana can explain its structural role in cross-linking and strengthening of plant cell wall polysaccharides (Russell

et al. 2009). The presence of ferulic acid in banana fruit and stem extracts has been consistently confirmed in numerous publications, with HPLC being the chosen method for its identification (Zainol et al. 2018). Furthermore, ferulic acid was successfully determined among other bioactive compounds in stem juices from banana plants using a tandem high-resolution mass spectrometry (UHPLC-HRMS/MS) method. An investigation into variations in the occurrence of potentially antidiabetic compounds revealed significant differences in the concentration of ferulic acid based on the origin of the bananas, underscoring the influence of growth conditions on its presence (Nguyen et al. 2017). Phenolic compound profiling in various banana varieties was also conducted through two analytical methods, HPLC–ESI-HR-MS and HPLC-DAD. The research findings demonstrated that bananas serve as a rich source of phenolic compounds; however, their content exhibits variations between the pulp and peel of this fruit (Passo Tsamo et al. 2015).

The remarkable antioxidant properties of bananas can be attributed to the presence of various phenolic compounds, including sinapic acid. Similar to ferulic acid, sinapic acid is a derivative of cinnamic acid and is predominantly found in the outer region of the pulp near the peel (Fig. 1K). Sinapic acid has been identified through LC MS/MS analysis in banana roots (Shi Ming et al. 2021). Furthermore, it has been observed that sinapic acid levels increase in bananas treated with artificial ripeners (Tallapally et al. 2020). Previous research on extracts from different morphological parts of bananas indicated that ferulic acid is more abundant in leaf sheaths and floral stalks, whereas rachis contains it in smaller quantities (Oliveira et al. 2006).

Quercetin, catechin, and myricetin are prominent members of the flavonoid family, renowned for their robust antioxidant activity. These naturally occurring phenols and secondary metabolites are widespread among various plants. Structurally, they share similarities and belong to the flavonol class of flavonoids, exhibiting numerous common functions. In our study, all three compounds were detected in close proximity to the fibrovascular bundles (Fig. 1M, N, O). Flavonoids serve vital roles as secondary metabolites synthesized by plants, contributing to various functions, including stress defense, pigmentation, and attraction of pollinators or seed dispersers (Buer et al. 2010). In the context of fruits, flavonoids play a crucial role in pigmentation and safeguarding against environmental factors (Harborne and Williams 2000). The strategic location of flavonoids like quercetin, catechin, and myricetin near fibrovascular bundles can be attributed to their specific transport and localization patterns. Fibrovascular bundles play a pivotal role in facilitating substance movement within fruits, ensuring the efficient distribution of flavonoids to regions where they are needed (Quattrocchio et al. 2006). This localization in proximity to fibrovascular bundles ensures the availability of flavonoids for protective and pigmentation purposes, contributing to the overall health and resilience of the banana fruit. The antioxidant properties of polyphenols such as quercetin, catechin, and myricetin in bananas have been extensively researched. Notably, in a study comparing 15 commonly consumed fruits and vegetables, bananas were found to have the highest phenolic content (Singh et al. 2016a). Catechin has been identified as the primary constituent in both banana peel (Someya et al. 2002) and pulp (Bennett et al. 2010) extracts. Additionally, quercetin has been detected in bananas using UPLC-MS analysis (Septembre-Malaterre et al. 2016). These findings highlight the significant presence of these beneficial polyphenols in bananas and underscore their potential health-promoting effects.

Flavonoids, such as flavanols like quercetin and myricetin, have been successfully identified in the sap of various dessert banana species using HPLC-ESI-MS (Pothavorn et al. 2010). Both quercetin and catechin have been detected in the banana pulp at all stages of fruit development. Among the flavonoids, quercetin emerged as the predominant metabolite in its free soluble form in bananas (Dong et al. 2016a). Furthermore, myricetin has been previously reported in extracts from the banana peel (Zhang et al. 2019).

In this study, pyruvic acid was identified as the compound with the lowest molecular weight, using the LARESI method, and was found in the pulp close to the center of the banana fruit (Fig. 1D, E). Pyruvic acid is a three-carbon carboxylic acid containing both a ketone and a carboxyl functional group. Its significance lies in its crucial role as an intermediate in various metabolic pathways within the cell, including those involving lipids, amino acids, and carbohydrates. In the cell's environment, pyruvic acid dissociates into pyruvate ions (pyruvate). It is produced during glycolysis, where glucose molecules are broken down into two pyruvate ions. Subsequently, in the mitochondria's matrix, pyruvate is converted into acetyl coenzyme A (acetyl CoA), which further participates in the energy-supplying citric acid cycle (Krebs cycle) when oxygen is present. In the absence of oxygen, pyruvate ferments into lactate (lactic acid). Moreover, pyruvate can be converted into alanine via transamination or into oxaloacetate through carboxylation. Previous studies have quantified pyruvic acid in banana pulp extracts using gas-liquid chromatography (GLC) (McHan and Horvat 1987) and high-performance liquid chromatography (HPLC) (Kozukue 1981). These studies also revealed that the level of pyruvic acid slightly decreased during ripening after five months of storing bananas at −20°C. However, the isolation, separation, and identification of pyruvic acid, like other α-keto acids in biological materials, pose challenges due to their instability.

Isobutyl butyrate, a carboxylic acid ester, is a volatile compound that is produced during the ripening of banana fruits. Its identification and quantification in bananas have

been extensively studied due to its significant impact on fruit and flavor quality, employing various analytical methods. In our experiment, isobutyl butyrate was detected in the banana pulp, with the highest intensity of the signal observed near the fibrovascular bundles (Fig. 1F). The quantification of isobutyl butyrate in commercial banana fruit and banana essence was achieved using GC-MS (Jordán et al. 2001). This aromatic compound was identified at two stages of banana ripening: during the color-turning and full-ripening stages, using the solid-phase micro-extraction (SPME) coupled with the GS-MS method (Zhu et al. 2018). Moreover, studies on bananas harvested in different seasons demonstrated that only fruits harvested in March contained isobutyl butyrate and exhibited a higher abundance of volatile aroma compounds (Zhang et al. 2020).

Another notable volatile compound in bananas is eugenol, which belongs to the naturally occurring phenylpropanoid class of organic aromatic compounds, featuring a propylbenzene skeleton. Similar to other secondary metabolites, eugenol was also found in close proximity to the fibrovascular bundles (Fig. 1H). It is associated with a phenolic, sweet flavor, contributing to the overall sensory profile of bananas. Eugenol, a significant flavor compound, has been identified in high concentrations in fresh banana fruit paste, banana extracts, and dehydrated banana powder, utilizing various methods coupled with GC-MS (Miranda et al. 2001; Wang et al. 2007; Pino and Febles 2013). Intriguingly, eugenol was not detected in commercial banana essence, highlighting the distinct aromatic profiles between fresh fruit and banana essence (Jordán et al. 2001). It is noteworthy that the flavor compounds in banana extracts are not formed during the growth and time of harvest, but rather during the ripening process of the fruit (Boudhrioua et al. 2003). This implies that the development of characteristic flavors in bananas is a dynamic process, occurring primarily during the ripening stage, which significantly influences the overall sensory experience of consuming this fruit.

In the second experiment, the spatial distribution of 16 amino acids (AAs) in Red Dacca Banana tissue was examined. AAs play several important roles in banana fruit. As essential nutrients, AAs are essential building blocks for protein synthesis, which is crucial for the growth, development, and maintenance of the fruit. Proteins are essential components of various cellular structures and enzymes that regulate biochemical processes within the fruit. Additionally, amino acids are involved in various metabolic pathways within the banana fruit. They participate in energy production through processes like glycolysis and the citric acid cycle (TCA cycle), providing the necessary energy for cellular activities during fruit ripening and development (Wiskich and Dry 1985). AAs also contribute to the flavor and aroma of banana fruit. Certain amino acids are precursors to volatile compounds, which are responsible for the characteristic scent and taste of ripe bananas (Maoz et al. 2022). Furthermore, AAs play a role in stress responses and defense mechanisms in the fruit. During postharvest senescence, amino acids may be utilized to protect the fruit from oxidative damage and maintain cellular integrity (He et al. 2013). The majority of the tested AAs were found in the pulp of the fruit, with the exception of three amino acids, threonine, methionine, and cysteine, which were also present in the peel (Fig. 2G, 2L, 2R). Notably, cysteine accumulated mainly in the outer part of the banana peel, with only a negligible amount detected in the pulp. Furthermore, MS imaging revealed a high content of exogenous amino acids on the entire surface of the banana, such as valine, tryptophan, histidine, and phenylalanine, with their accumulation predominantly occurring between the peel and the pulp. In contrast, the lowest intensities in ionic images were observed for asparagine, lysine, and arginine. These amino acids possess additional amino groups in their side chains, which may contribute to their distribution pattern within the banana tissues. Our findings align with prior studies that shed light on the distribution of threonine, glutamine, and arginine within banana pulps during postharvest senescence (Yin et al. 2022). These studies revealed that these AAs exclusively accumulated in the middle region near the seed zone.

Conclusions

Utilizing mass spectrometry imaging (MSI) for banana analysis offered a detailed visualization of metabolites like antioxidants within the fruit's tissue, providing essential spatial data that traditional GC/LC-MS methods lack. This insight is valuable for research and enhancing food technology. MSI's minimal preparation preserves the integrity of sensitive compounds, avoiding the alterations extraction can cause. As a label-free approach, it detects antioxidants in their true form and delivers both qualitative and quantitative insights rapidly, without the sequential steps needed for individual compound analysis. By analyzing compounds directly in the tissue, MSI also minimizes the risk of compound loss or alteration inherent in conventional extraction techniques. Our research aimed to demonstrate the significant advantages of employing the LARESI method in SRM modes for targeted MSI of LMWC in intact plant tissues. Through this innovative approach, we were able to gain valuable insights into the spatial distribution of various compounds within plant tissues. It was possible to identify and determine the spatial distribution of 12 metabolites and 16 amino acids. The spatial distribution some of these compounds found in bananas was presented for the first time. The results of the studies presented in this publication confirm that LARESI method's efficiency, simplicity, and ability to analyze intact samples without the need for additional coatings or complex

sample preparation make it a powerful tool for advancing our knowledge of plant metabolomics and its diverse applications.

Funding The study was supported by National Science Centre (Poland) research project SONATA BIS Number 2022/46/E/ST4/00016.

Data Availability The data that support the findings of this study is available from the corresponding author upon reasonable request.

Declarations

Competing Interests The authors declare no competing interests.

Declaration of Generative AI and AI-Assisted Technologies in the Writing Process During the preparation of this work, the author(s) used ChatGPT3 (OpenAI) in order to improve language and readability. After using this tool/service, the author(s) reviewed and edited the content as needed and take(s) full responsibility for the content of the publication.

References

Adão RC, Glória MBA (2005) Bioactive amines and carbohydrate changes during ripening of 'Prata' banana (Musa acuminata × M. balbisiana). Food Chem 90:705–711. https://doi.org/10.1016/J.FOODCHEM.2004.05.020

Araújo FDS, Vieira RL, Molano EPL et al (2017) Desorption electrospray ionization mass spectrometry imaging reveals chemical defense of Burkholderia seminalis against cacao pathogens. RSC Adv 7:29953–29958. https://doi.org/10.1039/C7RA03895J

Audinot JN, Philipp P, De Castro O et al (2021) Highest resolution chemical imaging based on secondary ion mass spectrometry performed on the helium ion microscope. Reports Prog Phys 84:105901. https://doi.org/10.1088/1361-6633/AC1E32

Bartels B, Svatoš A (2015) Spatially resolved in vivo plant metabolomics by laser ablation-based mass spectrometry imaging (MSI) techniques: LDI-MSI and LAESI. Front Plant Sci 6:1–7. https://doi.org/10.3389/FPLS.2015.00471

Bennett RN, Shiga TM, Hassimotto NMA et al (2010) Phenolics and antioxidant properties of fruit pulp and cell wall fractions of postharvest banana (Musa acuminata Juss.) cultivars. J Agric Food Chem 58:7991–8003. https://doi.org/10.1021/JF1008692

Boudhrioua N, Giampaoli P, Bonazzi C (2003) Changes in aromatic components of banana during ripening and air-drying. LWT - Food Sci Technol 36:633–642. https://doi.org/10.1016/S0023-6438(03)00083-5

Brauer JI, Beech IB, Sunner J (2015) Mass spectrometric imaging using laser ablation and solvent capture by aspiration (LASCA). J Am Soc Mass Spectrom 26:1538–1547. https://doi.org/10.1007/S13361-015-1176-0

Buer CS, Imin N, Djordjevic MA (2010) Flavonoids: new roles for old molecules. J Integr Plant Biol 52:98–111. https://doi.org/10.1111/J.1744-7909.2010.00905.X

Cabral EC, Mirabelli MF, Perez CJ, Ifa DR (2013) Blotting assisted by heating and solvent extraction for DESI-MS imaging. J Am Soc Mass Spectrom 24:956–965. https://doi.org/10.1007/S13361-013-0616-Y

Calvano CD, Monopoli A, Cataldi TRI, Palmisano F (2018) MALDI matrices for low molecular weight compounds: an endless story? Anal Bioanal Chem 410:4015–4038. https://doi.org/10.1007/S00216-018-1014-X

Caprioli RM, Farmer TB, Gile J (1997) Molecular imaging of biological samples: localization of peptides and proteins using MALDI-TOF MS. Anal Chem 69:4751–4760. https://doi.org/10.1021/AC970888I

Chaurand P, Schwartz SA, Billheimer D et al (2004) Integrating histology and imaging mass spectrometry. Anal Chem 76:1145–1155. https://doi.org/10.1021/AC0351264

Cornett DS, Reyzer ML, Chaurand P, Caprioli RM (2007) MALDI imaging mass spectrometry: molecular snapshots of biochemical systems. Nat Methods 4(10):828–833. https://doi.org/10.1038/nmeth1094

da Silva LG, Franco dos Santos G, Ramalho RRF et al (2022) Laser ablation electrospray ionization mass spectrometry imaging as a new tool for accessing patulin diffusion in mold-infected fruits. Food Chem 373:131490. https://doi.org/10.1016/J.FOODCHEM.2021.131490

Dong C, Hu H, Hu Y, Xie J (2016a) Metabolism of flavonoids in novel banana germplasm during fruit development. Front Plant Sci 0:1291. https://doi.org/10.3389/FPLS.2016.01291

Dong Y, Li B, Malitsky S et al (2016b) Sample preparation for mass spectrometry imaging of plant tissues: A review. Front Plant Sci 7:170331. https://doi.org/10.3389/FPLS.2016.00060

dos Santos FN, Tata A, Belaz KRA et al (2017) Major phytopathogens and strains from cocoa (Theobroma cacao L.) are differentiated by MALDI-MS lipid and/or peptide/protein profiles. Anal Bioanal Chem 409:1765–1777. https://doi.org/10.1007/S00216-016-0133-5

Dou TX, Shi JF, Li Y et al (2020) Influence of harvest season on volatile aroma constituents of two banana cultivars by electronic nose and HS-SPME coupled with GC-MS. Sci Hortic 265:109214. https://doi.org/10.1016/J.SCIENTA.2020.109214

Eswara S, Pshenova A, Yedra L et al (2019) Correlative microscopy combining transmission electron microscopy and secondary ion mass spectrometry: a general review on the state-of-the-art, recent developments, and prospects. Appl Phys Rev 6:21312. https://doi.org/10.1063/1.5064768

Gao SQ, Zhao JH, Guan Y et al (2023) Mass spectrometry imaging technology in metabolomics: a systematic review. Biomed Chromatogr 37:e5494. https://doi.org/10.1002/BMC.5494

Gedük AŞ, Zengin F (2021) LC–MS/MS characterization, antidiabetic, antioxidative, and antibacterial effects of different solvent extracts of Anamur banana (Musa Cavendishii). Food Sci Biotechnol 30:1183–1193. https://doi.org/10.1007/S10068-021-00953-5

Goodwin RJA (2012) Sample preparation for mass spectrometry imaging: small mistakes can lead to big consequences. J Proteomics 75:4893–4911. https://doi.org/10.1016/J.JPROT.2012.04.012

Harborne JB, Williams CA (2000) Advances in flavonoid research since 1992. Phytochemistry 55:481–504. https://doi.org/10.1016/S0031-9422(00)00235-1

He S, Shan W, Kuang JF et al (2013) Molecular characterization of a stress-response bZIP transcription factor in banana. Plant Cell Tissue Organ Cult 113:173–187. https://doi.org/10.1007/S11240-012-0258-Y

Hölscher D, Fuchser J, Knop K et al (2015) High resolution mass spectrometry imaging reveals the occurrence of phenylphenalenone-type compounds in red paracytic stomata and red epidermis tissue of Musa acuminata ssp. zebrina cv. 'Rowe Red'. Phytochemistry 116:239–245. https://doi.org/10.1016/J.PHYTOCHEM.2015.04.010

Hussein Z, Fawole OA, Opara UL (2020) Harvest and postharvest factors affecting bruise damage of fresh fruits. Hortic Plant J 6:1–13. https://doi.org/10.1016/J.HPJ.2019.07.006

Joignant AN, Xi Y, Muddiman DC (2023) Impact of wavelength and spot size on laser depth of focus: considerations for mass spectrometry imaging of non-flat samples. J Mass Spectrom 58:e4914. https://doi.org/10.1002/JMS.4914

Jordán MJ, Tandon K, Shaw PE, Goodner KL (2001) Aromatic profile of aqueous banana essence and banana fruit by gas chromatography-mass spectrometry (GC-MS) and gas chromatography-olfactometry (GC-O). J Agric Food Chem 49:4813–4817. https://doi.org/10.1021/JF010471K

Kandasamy S, Aradhya SM (2014) Polyphenolic profile and antioxidant properties of rhizome of commercial banana cultivars grown in India. Food Biosci 8:22–32. https://doi.org/10.1016/J.FBIO.2014.10.001

Kaspar S, Peukert M, Svatos A et al (2011) MALDI-imaging mass spectrometry – an emerging technique in plant biology. Proteomics 11:1840–1850. https://doi.org/10.1002/PMIC.201000756

Kozukue N (1981) Determination of alpha-keto acids in banana pulp by high performance liquid chromatography. J Food Sci 46:156–160. https://doi.org/10.1111/j.1365-2621.1981.tb14552.x

Li Y, Shrestha B, Vertes A (2007) Atmospheric pressure molecular imaging by infrared MALDI mass spectrometry. https://doi.org/10.1021/AC061577N

Lima GPP, Da Rocha SA, Takaki M et al (2008) Comparison of polyamine, phenol and flavonoid contents in plants grown under conventional and organic methods. Int J Food Sci Technol 43:1838–1843. https://doi.org/10.1111/J.1365-2621.2008.01725.X

Maduwanthi SDT, Marapana RAUJ (2021) Total phenolics, flavonoids and antioxidant activity following simulated gastro-intestinal digestion and dialysis of banana (Musa acuminata, AAB) as affected by induced ripening agents. Food Chem 339:127909. https://doi.org/10.1016/J.FOODCHEM.2020.127909

Maoz I, Lewinsohn E, Gonda I (2022) Amino acids metabolism as a source for aroma volatiles biosynthesis. Curr Opin Plant Biol 67:102221. https://doi.org/10.1016/J.PBI.2022.102221

McDonnell LA, Heeren RMA (2007) Imaging mass spectrometry. Mass Spectrom Rev 26:606–643. https://doi.org/10.1002/MAS.20124

McHan F, Horvat RJ (1987) Insoluble monolayers at liquid-gas interfaces. In: Kinsella JE, Damodaran S (eds) In Criteria of Food Acceptance, vol 35, pp 453–461 American Chemical Society

Miranda EJF, Nogueira RI, Pontes SM, Rezende CM (2001) Odour-active compounds of banana passa identified by aroma extract dilution analysis. Flavour Fragr J 16:281–285. https://doi.org/10.1002/FFJ.997

Misiorek M, Sekuła J, Ruman T (2017) Mass spectrometry imaging of low molecular weight compounds in garlic (Allium sativum L.) with gold nanoparticle enhanced target. Phytochem Anal 28:479–486. https://doi.org/10.1002/PCA.2696

Mondal A, Banerjee S, Bose S et al (2021) Cancer preventive and therapeutic potential of banana and its bioactive constituents: a systematic, comprehensive, and mechanistic review. Front Oncol 11:697143. https://doi.org/10.3389/FONC.2021.697143

Nguyen D, Nováková A, Spurná K et al (2017) Antidiabetic compounds in stem juice from banana. Czech J Food Sci 35:407–413. https://doi.org/10.17221/172/2017-CJFS

Nizioł J, Sekuła J, Ruman T (2017) Visualizing spatial distribution of small molecules in the rhubarb stalk (Rheum rhabarbarum) by surface-transfer mass spectrometry imaging. Phytochemistry 139. https://doi.org/10.1016/j.phytochem.2017.04.006

Nizioł J, Sunner J, Beech I et al (2020) Localization of metabolites of human kidney tissue with infrared laser-based selected reaction monitoring mass spectrometry imaging and Silver-109 nanoparticle-based surface assisted laser desorption/ionization mass spectrometry imaging. Anal Chem 92:4251–4258. https://doi.org/10.1021/ACS.ANALCHEM.9B04580

Norris JL, Caprioli RM (2013) Analysis of tissue specimens by matrix-assisted laser desorption/ionization imaging mass spectrometry in biological and clinical research. Chem Rev 113:2309–2342. https://doi.org/10.1021/CR3004295

Oliveira L, Freire CSR, Silvestre AJD et al (2006) Lipophilic extractives from different morphological parts of banana plant "Dwarf Cavendish". Ind Crops Prod 23:201–211. https://doi.org/10.1016/J.INDCROP.2005.06.003

Passo Tsamo CV, Herent MF, Tomekpe K et al (2015) Effect of boiling on phenolic profiles determined using HPLC/ESI-LTQ-Orbitrap-MS, physico-chemical parameters of six plantain banana cultivars (Musa sp). J Food Compos Anal 44:158–169. https://doi.org/10.1016/J.JFCA.2015.08.012

Pino JA, Febles Y (2013) Odour-active compounds in banana fruit cv. Giant Cavendish. Food Chem 141:795–801. https://doi.org/10.1016/J.FOODCHEM.2013.03.064

Pothavorn P, Kitdamrongsont K, Swangpol S et al (2010) Sap phytochemical compositions of some bananas in Thailand. J Agric Food Chem 58:8782–8787. https://doi.org/10.1021/JF101220K

Qamar S, Shaikh A (2018) Therapeutic potentials and compositional changes of valuable compounds from banana- a review. Trends Food Sci Technol 79:1–9. https://doi.org/10.1016/J.TIFS.2018.06.016

Quattrocchio F, Baudry A, Lepiniec L, Grotewold E (2006) The regulation of flavonoid biosynthesis. Sci Flavonoids:97–122. https://doi.org/10.1007/978-0-387-28822-2_4/COVER

Rocha DFO, Cunha CMS, Belaz KRA et al (2017) Lipid and protein fingerprinting for Fusarium oxysporum f. sp. cubense strain-level classification. Anal Bioanal Chem 409:6803–6812. https://doi.org/10.1007/S00216-017-0638-6

Russell JB, Muck RE, Weimer PJ (2009) Quantitative analysis of cellulose degradation and growth of cellulolytic bacteria in the rumen. FEMS Microbiol Ecol 67:183–197. https://doi.org/10.1111/J.1574-6941.2008.00633.X

Sarabia LD, Boughton BA, Rupasinghe T et al (2018) High-mass-resolution MALDI mass spectrometry imaging reveals detailed spatial distribution of metabolites and lipids in roots of barley seedlings in response to salinity stress. Metabolomics 14:1–16. https://doi.org/10.1007/S11306-018-1359-3

Saravanan K, Aradhya SM (2011) Polyphenols of pseudostem of different banana cultivars and their antioxidant activities. J Agric Food Chem 59:3613–3623. https://doi.org/10.1021/jf103835z

Septembre-Malaterre A, Stanislas G, Douraguia E, Gonthier M-P (2016) Evaluation of nutritional and antioxidant properties of the tropical fruits banana, litchi, mango, papaya, passion fruit and pineapple cultivated in Réunion French Island. https://doi.org/10.1016/j.foodchem.2016.05.147

Shi Ming F, Razali Z, Somasundram C (2021) Involvement of phenolic compounds and their composition in the defense response of Fusarium oxysporum infected Berangan banana plants. Sains Malays 50:23–33. https://doi.org/10.17576/jsm-2021-5001-03

Sidhu JS, Zafar TA (2018) Bioactive compounds in banana fruits and their health benefits. Food Qual Saf 2:183–188. https://doi.org/10.1093/FQSAFE/FYY019

Silva VDM, Arquelau PBF, Silva MR et al (2020) Use of paper spray-mass spectrometry to determine the chemical profile of ripe banana peel flour and evaluation of its physicochemical and antioxidant properties. Quim Nova 43:579–585. https://doi.org/10.21577/0100-4042.20170521

Simirgiotis MJ, Schmeda-Hirschmann G, Bórquez J, Kennelly EJ (2013) The *Passiflora tripartita* (banana passion) fruit: a source of bioactive flavonoid C-glycosides isolated by HSCCC and characterized by HPLC–DAD–ESI/MS/MS. Molecules 18(2):1672–1692. https://doi.org/10.3390/MOLECULES18021672

Singh B, Singh JP, Kaur A, Singh N (2016b) Bioactive compounds in banana and their associated health benefits – a review. Food Chem 206:1–11. https://doi.org/10.1016/J.FOODCHEM.2016.03.033

Singh J, Kaur A, Shevkani K, Singh N (2016a) Composition, bioactive compounds and antioxidant activity of common Indian fruits and vegetables. J Food Sci Technol 53:4056–4066. https://doi.org/10.1007/S13197-016-2412-8

Someya S, Yoshiki Y, Okubo K (2002) Antioxidant compounds from bananas (Musa Cavendish). Food Chem 79:351–354. https://doi.org/10.1016/S0308-8146(02)00186-3

Stoeckli M, Chaurand P, Hallahan DE, Caprioli RM (2001) Imaging mass spectrometry: a new technology for the analysis of protein expression in mammalian tissues. Nat Med 7(4):493–496. https://doi.org/10.1038/86573

Szulc J, Ruman T (2020) Laser ablation remote-electrospray ionisation mass spectrometry (LARESI MSI) imaging—new method for detection and spatial localization of metabolites and mycotoxins produced by moulds. Toxins 12(11):720. https://doi.org/10.3390/TOXINS12110720

Tallapally M, Sadiq AS, Mehtab V et al (2020) GC-MS based targeted metabolomics approach for studying the variations of phenolic metabolites in artificially ripened banana fruits. LWT 130:109622. https://doi.org/10.1016/J.LWT.2020.109622

Tata A, Perez CJ, Hamid TS et al (2015) Analysis of metabolic changes in plant pathosystems by imprint imaging desi-ms. J Am Soc Mass Spectrom 26:641–648. https://doi.org/10.1007/S13361-014-1039-0

Tongkaew P, Tohraman A, Bungaramphai R et al (2022) Kluai Hin (*Musa sapientum* Linn.) peel as a source of functional polyphenols identified by HPLC-ESI-QTOF-MS and its potential antidiabetic function. Sci Rep 12:1–8. https://doi.org/10.1038/s41598-022-08008-3

Vu HT, Scarlett CJ, Vuong QV (2018) Phenolic compounds within banana peel and their potential uses: a review. J Funct Foods 40:238–248. https://doi.org/10.1016/J.JFF.2017.11.006

Wang J, Li YZ, Chen RR et al (2007) Comparison of volatiles of banana powder dehydrated by vacuum belt drying, freeze-drying and air-drying. Food Chem 104:1516–1521. https://doi.org/10.1016/J.FOODCHEM.2007.02.029

Wiskich JT, Dry IB (1985) The tricarboxylic acid cycle in plant mitochondria: its operation and regulation. Higher Plant Cell Respiration:281–313. https://doi.org/10.1007/978-3-642-70101-6_11

Wu C, Dill AL, Eberlin LS et al (2013a) Mass spectrometry imaging under ambient conditions. Mass Spectrom Rev 32:218–243. https://doi.org/10.1002/MAS.21360

Wu X, Qin R, Wu H et al (2020) Nanoparticle-immersed paper imprinting mass spectrometry imaging reveals uptake and translocation mechanism of pesticides in plants. Nano Res 13:611–620. https://doi.org/10.1007/s12274-020-2700-5

Xiao Y, Deng J, Yao Y et al (2020) Recent advances of ambient mass spectrometry imaging for biological tissues: a review. Anal Chim Acta 1117:74–88. https://doi.org/10.1016/J.ACA.2020.01.052

Yin R, Kyle J, Burnum-Johnson K et al (2018) High spatial resolution imaging of mouse pancreatic islets using nanospray desorption electrospray ionization mass spectrometry. Anal Chem 90:6548–6555. https://doi.org/10.1021/acs.analchem.8b00161

Yin Z, Dong T, Huang W et al (2022) Spatially resolved metabolomics reveals variety-specific metabolic changes in banana pulp during postharvest senescence. Food Chem X 15:100371. https://doi.org/10.1016/J.FOCHX.2022.100371

Yoshimura Y, Goto-Inoue N, Moriyama T, Zaima N (2016) Significant advancement of mass spectrometry imaging for food chemistry. Food Chem 210:200–211. https://doi.org/10.1016/J.FOODCHEM.2016.04.096

Yun Z, Gao H, Chen X et al (2022) The role of hydrogen water in delaying ripening of banana fruit during postharvest storage. Food Chem 373:131590. https://doi.org/10.1016/J.FOODCHEM.2021.131590

Zainol N, Masngut N, Jusup MK (2018) Kinetic study on ferulic acid production from banana stem waste via mechanical extraction. IOP Conf Ser Mater Sci Eng 342:012038. https://doi.org/10.1088/1757-899X/342/1/012038

Zduńska K, Dana A, Kolodziejczak A, Rotsztejn H (2018) Antioxidant properties of ferulic acid and its possible application. Skin Pharmacol Physiol 31:332–336. https://doi.org/10.1159/000491755

Zhang JW, Wang JH, Wang GH et al (2019) Extraction and characterization of phenolic compounds and dietary fibres from banana peel. Acta Aliment 48:525–537. https://doi.org/10.1556/066.2019.48.4.14

Zhang XW, Li QH, Di XZ, Dou JJ (2020) Mass spectrometry-based metabolomics in health and medical science: a systematic review. RSC Adv 10:3092–3104. https://doi.org/10.1039/C9RA08985C

Zhu X, Li Q, Li J et al (2018) Comparative study of volatile compounds in the fruit of two banana cultivars at different ripening stages. Molecules 23(10):2456. https://doi.org/10.3390/MOLECULES23102456

Zou Y, Tang W, Li B (2022) Mass spectrometry imaging and its potential in food microbiology. Int J Food Microbiol 371:109675. https://doi.org/10.1016/J.IJFOODMICRO.2022.109675